nature physics

SUPPLEMENTARY INFORMATION

DOI: 10.1038/NPHYS2924

Ferroelectric quantum criticality

S. E. Rowley[1,2,3], L. J. Spalek[1], R. P. Smith[1], M. P. M. Dean[1,4], M. Itoh[5], J. F. Scott[1], G. G. Lonzarich[1] and S. S. Saxena[1]

1. *Cavendish Laboratory, University of Cambridge, J.J. Thomson Avenue, Cambridge, CB3 0HE, U.K.*
2. *Department of Physics, Princeton University, Princeton, New Jersey 08544, U.S.A.*
3. *Centro Brasileiro de Pesquisas Físicas, Rua Dr Xavier Sigaud 150, Rio de Janeiro, 22290-180, Brazil*
4. *Condensed Matter Physics and Materials Science Department, Brookhaven National Laboratory, Upton, New York, 11973, USA*
5. *Materials & Structures Laboratory, Tokyo Institute of Technology, 4259 Nagatsuta, Midori, Yokohama 226-8503, Japan*

A) Experimental Details

Measurements of the dielectric function $\varepsilon(T)$ versus temperature were carried out in a number of specimens of $SrTiO_3$ and $KTaO_3$ of varying purities and grown via different techniques to check for the consistency of our results[1]. All our samples were single crystals, cut into rectangular cuboids of approximate dimensions 5 mm × 5 mm × 0.3 mm. The crystal structure of $KTaO_3$ is known to remain cubic down to the lowest temperatures measured in the millikelvin range. The crystal structure of $SrTiO_3$ is cubic down to 105 K and remains approximately cubic, although with a slight tetragonal distortion below 105 K, insufficient in strength to significantly affect our analyses[2-4]. Dielectric measurements were carried out in the parallel plate capacitance geometry using gold electrodes on the large surfaces. Two cryostats, an adiabatic demagnetisation refrigerator (0.04 K to 300 K) and a pumped helium-3 system (0.3 K to 300 K) both fitted with miniature coaxial cables, were used for high precision signal detection with an Andeen-Hagerling, QuadTech and Agilent capacitance bridges. Measurements were taken during heating at a rate of less than 1 K per hour at low temperatures and approximately 5 K per hour at high temperatures. The frequency could be varied from a few Hz to a few MHz and a low noise DC field could be varied between 0 and 20 kV/cm during measurements. The temperature was measured to an accuracy of better than 1% and the dielectric function to a relative accuracy of better than 0.01%.

B) Origin of Non-Classical Critical Exponents

An elementary derivation of the critical exponent γ defined in Table 2 in the main text may be given as follows (see Section C for a more complete treatment). We assume that in the static limit at absolute zero the relation between the order parameter and its conjugate field, e.g., the electric polarization P and the electric field E, is of the analytic form $\varepsilon_0 E = aP + bP^3 -$

DOI: 10.1038/NPHYS2924

$c\nabla^2 P$ for small fields and long wavelengths, where a, b and c are positive parameters under our experimental conditions. In this equation a is the inverse static susceptibility, b is the mode-mode coupling parameter and c is the mode stiffness parameter defined in terms of the basic parameter set (a, b, Δ, v) in Table I by $c = a\, v^2/\Delta^2$, in the $T = 0$ K limit as in the paraelectric phase where $a > 0$. The renormalization of these parameters with temperature may be obtained by taking a thermal average of the equation of state in the presence of a random (Langevin) field of zero mean which is imagined to drive the thermal and quantum fluctuations in P. This leads to a non-vanishing contribution from the cubic (anharmonic) term so that up to second order in a cumulant expansion of the thermal average of P^3

$$\varepsilon_0 E = (a + g_1 \mathrm{var}P)\overline{P} + b\overline{P}^3 - c\nabla^2\overline{P}$$

where $\overline{P}$ is the average polarization stabilized by E, $varP$ is the thermal variance of the local polarization (suitably coarse grained as defined below) and g_1 is a numerical factor which depends on the number of relevant components of the polarization vector. g_1 is equal to three in the special case of a purely scalar field. The value of g_1 appropriate to the present work is implicitly defined under Section C taking into account the effects of the long-range dipolar interaction in the manner discussed in the main text. The variance of P can be expressed via the fluctuation-dissipation theorem approximately as

$$\mathrm{var}P = k_B T \hat{\sum_{q<q_T}} \chi_q[\overline{P}]$$

where the sum $\hat{\Sigma}$ is per unit volume, χ_q is the electric susceptibility in the presence of $\overline{P}$, and q_T is a thermal cut-off defined by the condition that ω_{q_T} (or Γ_{q_T}) is approximately equal to $k_B T/\hbar$. An expansion of $varP$ in a power series in $\overline{P}$ and $\nabla^2\overline{P}$ leads to the thermal renormalization of the coefficients of the linear, cubic and gradient terms in the equation of state. In particular, the inverse wavevector dependent susceptibility at finite T is then

$$1/\chi_q(T) = \left(a + g_1 b k_B T \sum_{q<q_T} \chi_q\right) + cq^2$$

in the limit of vanishing $\overline{P}$ (and hence vanishing electric field E). We have retained only the thermal correction which is expected to dominate near to the quantum critical point where a tends to zero. Setting a equal to zero, we then find that the square of the correlation wavevector, $\kappa^2(T) = 1/(\chi(T)c)$, satisfies the self-consistent equation

$$\kappa^2(T) = g_2 b k_B T \int_0^{q_T} \frac{q^{d-1} dq}{\kappa^2(T) + q^2}$$

where g_2 is a new numerical constant. If in leading order in T, $\kappa^2(T)$ on the rhs can be ignored then $\kappa^2 = g_2 b k_B T\, q_T^{d-2}/(d-2)$, so that if ω_q (or Γ_q) $\propto q^z$, we find $\kappa^2(T) \propto T^{(d+z-2)/z}$, which yields the expression for the quantum critical exponent γ given in the caption of Table 1 in the main text.

We note, however, that the neglect of κ^2 on the r.h.s. of the above integral is not valid if $d+z$ is below the upper critical or marginal dimension of 4. At this marginal dimension the retention of the κ^2 term on the r.h.s. can readily be seen to lead to a weak correction, logarithmic in T, to the above $T^{(d+z-2)/z}$ temperature dependence expected for $d + z > 4$. A renormalization group treatment is needed to obtain the correct form of this weak correction and, in particular, to describe the equation of state below the upper critical dimension in general[5,6].

The above result for the quantum critical exponent for the order parameter susceptibility is not specific to a displacive quantum paraelectric. For the latter case, which is characterized by $z = 1$, the quantum critical exponent γ can also be understood by noting (i) that the number of thermally excited quanta of the polarization field increases with T in proportion to the q-space volume q_T^d, and (ii) that, as in the case of a simple quantum oscillator, the efficiency of an excited quantum in changing the variance of the displacement is inversely proportional to the energy carried by the quantum. For our case ($z = 1$) this implies that the variance of the local displacement and hence polarization at low temperatures should vary as q_T^d/q_T, which is proportional to T^2 in three spatial dimensions, in agreement with the more detailed analyses given above and in Section C. At higher temperatures where the q-space volume of thermally activated modes saturates, the thermal population of quanta, as well as the variance of the local displacements or of the local polarization, increase linearly with T as required in the classical limit. The crossover from the low T to the high T behaviours is determined by the numerical analyses described under Section C and illustrated for realistic parameters for $SrTiO_3$ and $KTaO_3$ in the figures in the main text.

C) Detailed Theoretical Model

The calculations of the dielectric function $\varepsilon(T) = 1 + \chi(T)$ were carried out in terms of the self-consistent field approximation to the ϕ^4 field model for a simple displacive ferroelectric in three dimensions including the effects of the long range dipole interactions as explained in the main text (see section B for a qualitative discussion). In terms of the parameters defined

DOI: 10.1038/NPHYS2924

under Table I, $\chi(T)$ was determined from the self-consistent equation[1,7,8]

$$\kappa^2(T) = \kappa^2(0) + \xi \int dq\, q^2 \left[\sum_n \frac{T}{\kappa^2(T) + q^2 + \omega_n^2} - \frac{1}{2\pi} \int \frac{d\omega}{\kappa^2(0) + q^2 + \omega^2} \right]$$

where the wavevetor q and the correlation wavevector $\kappa(T)$ are in units of the relevant Debye wavevector Λ, T is in units of the relevant Debye temperature θ and $\omega_n = 2\pi nT$, where n is an integer. The cut-offs in wavevector and frequency are taken to be unity (i.e., $0 < q < 1$ and $-1 < \omega < 1$). The dimensionless correlation wavevector $\kappa(T)$ and the dimensionless coupling parameter ξ are given, in terms of the parameters in Table I, by

$$\kappa^2(T) = \frac{\Delta^2 \chi(0)}{v^2 \Lambda^2 \chi(T)} \qquad \text{and} \qquad \xi = \frac{5\varepsilon_0 \hbar b\, \Delta^4 \chi^2(0)}{3\pi^2 v^3}$$

For a displacive ferroelectric with $d = 3$ and $z = 1$ near to the quantum critical point where $a \to 0$, the low temperature form of $\chi(T)$ can be approximately expressed in closed form as follows in terms of parameters which are readily obtained from experiments (examples for $SrTiO_3$ and $KTaO_3$ are given in Table I).

$$1/\chi(T) = a + \frac{5\varepsilon_0 k_B^2 b}{18\hbar c v} T^2$$

In the weakly ferroelectric state where a is small, and negative, the condition $1/\chi(T_C) \to 0$ yields an expression for the Curie temperature of the form

$$k_B T_C = \left(\frac{18\hbar c v |a|}{5\varepsilon_0 b} \right)^{1/2}$$

where $c = |a| v^2 / \Delta^2$ in terms of the basic model parameters defined in the caption of Table I. These expressions in terms of the model parameters presented in Table I and in the caption of Figs. 4 and 5 (in the main text), provide a qualitative and approximate quantitative account of the observed behaviour of the inverse susceptibility and Curie temperature shown in Figs. 2, 3 and 5 in the main text. They may be readily used to anticipate and understand behaviour of other ferroelectrics tuned close to quantum critical points. A more detailed description involves using the numerical calculation explained at the beginning of this section C and the correction below to quantitatively understand the low temperature upturns in the inverse susceptibly as presented in the figures in the main text.

The coupling between the critical transverse optic mode and the acoustic mode leads to a correction to $\kappa^2(T)$ of the form (see, e.g., refs. 7,8)

$$\delta\kappa^2(T) = -\lambda \int dq\, q^2 \left[\sum_n \frac{T}{\left(\kappa^2(T) + q^2 + \omega_n^2\right)\left(q^2 + \eta^2\omega_n^2\right)} - \frac{1}{2\pi}\int \frac{d\omega}{\left(\kappa^2(0) + q^2 + \omega^2\right)\left(q^2 + \eta^2\omega^2\right)} \right]$$

where η is the ratio of v (defined in Table I) to the velocity of the acoustic mode and λ is a dimensionless electrostrictive coupling constant. We have estimated the latter via the strain dependence of the energy gap[9,10] of the order parameter mode that suggests

$$\lambda \approx \frac{3K\xi}{20\varepsilon_0 b p_c^2 \chi^2(0)}$$

where ξ is the dimensionless parameter defined above, K is the bulk modulus and p_c is the critical pressure (negative for $SrTiO_3$ and $KTaO_3$) where the $T = 0$ K correlation wavevector is expected to vanish. We note that the electrostrictive effect is also expected to make a negative contribution to the mode-coupling parameter, b, and lead potentially to a first order transition[7,8,11]. Numerical estimates suggest, however, that the transition should remain second order under our experimental conditions in agreement with measurements down to 0.3 K in both $SrTiO_3$ and $KTaO_3$. Nonetheless, as one approaches even closer to the quantum critical point than explored in our experiments, a sign change in b may occur.

Further possible corrections alluded to in the text, including an effect analogous to that in the illustrative ϕ^4 model considered by Coleman and Weinberg[12], appear to be absent or subdominant under the experimental conditions of the present study.

Finally, we comment that in the limit where κ^2 is comparable to or greater than q^2 in the above equations (for all $q < \Lambda$), and ignoring the electrostrictive coupling effect, our model tends to that obtained in the Einstein or independent ion approximation. This is where each oscillator is considered to vibrate with a fixed frequency. The non-self-consistent version of this approximation is sometimes referred to as the Barrett model[13] and in the past has been fitted to experimental data in ferroelectric materials. We find using independently measured and temperature independent parameters as defined in this letter that the Barrett model is insufficient to explain the non-classical temperature dependence of ε in the quantum critical regimes (Fig. 4 in the main text) of $SrTiO_3$, oxygen-18 substituted $SrTiO_3$ and $KTaO_3$. It is in the quantum critical regime that the frequencies of the modes are strongly wavevector and temperature dependent, effects not included in the Barrett model.

DOI: 10.1038/NPHYS2924

Table I Material specific parameters for $SrTiO_3$ and $KTaO_3$ in the zero temperature limit. The quantum ϕ^4 field model for a displacive ferroelectric is defined in terms of four parameters, a, b, Δ and v in the limit of absolute zero. The parameters a and b were obtained from the intercept and slope, respectively, of plots of $\varepsilon_0 E/P$ vs P^2 at 0.3K, where E is the electric field (0 to 15kV/cm in our measurements) and P is the electric polarization ($\varepsilon_0 E/P = a + bP^2$). The parameters v and Δ were determined by comparing the data from inelastic neutron[14,15] and Raman scattering[16] experiments at 4 K to an equation of the form $\omega_q^2 = \Delta^2 + v^2 q^2$, which defines the low q and low T dispersion in the paraelectric state of the transverse-optic phonons that are the soft modes of the incipient ferroelectric state. Note that $\Delta = v\kappa(0)$, where $\kappa(0) = \sqrt{c/a}$ is the zero-temperature correlation wavevector, c is the stiffness parameter defined in section B, and v reduces to a speed of sound in the $\Delta = 0$ limit. The relatively small values of a and Δ for $SrTiO_3$ and $KTaO_3$ imply that these materials are close to displacive ferroelectric quantum critical points. The dimensionless coupling constant ξ, defined in Section C, is approximately 0.8 for $SrTiO_3$ and 0.6 for $KTaO_3$. Also, we have set Λ to be equal to 1.3 nm^{-1} for both materials.

	a	b ($C^{-2}m^4$)	$\hbar\Delta/k_B$ (K)	v (ms^{-1})
$SrTiO_3$	5.1 x 10^{-5}	0.07	24	8100
$KTaO_3$	2.2 x 10^{-4}	0.07	36	5700

Figure I Temperature dependence of $1/\varepsilon(T)$ in $SrTiO_3$ with quenched disorder. The main figure gives an example of the observed change (from the limiting T -> 0 K value) of the inverse dielectric function versus the square of the temperature up to ~ 60 K in a sintered polycrystalline specimen. The full dielectric function as a function of temperature up to room temperature is shown in the inset. We find that the non-classical T^2 power law is relatively insensitive to quenched disorder that is inevitably present in sintered or doped samples.

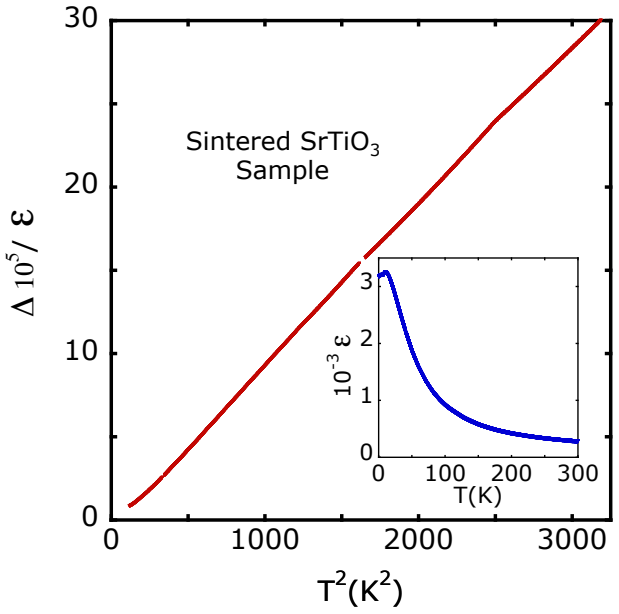

References

1 Rowley, S. E. *Quantum Phase Transitions in Ferroelectrics* (Ph.D. thesis, University of Cambridge, 2010).
2 Lytle, F. W. X-Ray diffractometry of low-temperature phase transformations in strontium titanate. *J. Appl. Phys.* **35**, 2212 (1964).
3 Fleury, P. A., Scott, J. F. & Worlock, J. M. Soft phonon modes and 110 degrees K phase transition in SrTiO3. *Phys. Rev. Lett.* **21**, 16-19 (1968).
4 Sakudo, T. & Unoki, H. Dielectric properties of SrTiO3 at low temperatures. *Phys. Rev. Lett.* **26**, 851-853 (1971).
5 Khmelnitskii, D. E. & Shneerson, V. L. Phase transition of the displacement type in crystals at very low temperature. *Sov. Phys. JETP* **37**, 164-170 (1973).
6 Roussev, R. & Millis, A. J. Theory of the quantum paraelectric-ferroelectric transition. *Phys. Rev. B* **67**, 014105 (2003).
7 Khmelnitskii, D. E. & Shneerson, V. L. Low-temperature displacement-type phase transition in crystals. *Sov. Phys. - Solid State* **13**, 687 (1971).
8 Palova, L., Chandra, P. & Coleman, P. Quantum critical paraelectrics and the Casimir effect in time. *Phys. Rev. B* **79**, 075101 (2009).
9 Uwe, H. & Sakudo, T. Stress induced ferroelectricity and soft phonon modes in SrTiO3. *Phys. Rev. B* **13**, 271-286 (1976).
10 Uwe, H. & Sakudo, T. Electrostriction and stress-induced ferroelectricity in KTaO3. *J. Phys. Soc. Japan* **38**, 183-189 (1975).
11 Larkin, A. J. & Pikin, S. A. On phase transitions of the first order resembling those of the second order. *Sov. Phys. JETP* **29**, 891-896 (1969).
12 Coleman, S. & Weinberg, E. Radiative-corrections as origin of spontaneous symmetry breaking. *Phys. Rev. D* **7**, 1888-1910 (1973).
13 Barrett, J. H. Dielectric constant in perovskite type crystals. *Phys. Rev.* **86**, 118-120 (1952).
14 Yamada, Y. & Shirane, G. Neutron scattering and nature of the soft optical phonon in SrTiO3. *J. Phys. Soc. Japan* **26**, 396-403 (1969).
15 Shirane, G., Nathans, R. & Minkiewicz, V. J. Temperature dependence of the soft ferroelectric mode in KTaO3. *Phys. Rev.* **157**, 396-399 (1967).
16 Fleury, P. A. & Warlock, J. M. Electric-field-induced Raman scattering in SrTiO3 and KTaO3. *Phys. Rev.* **174**, 613-623 (1968).